

1 | **Supergene formation is associated with a major shift in genome-wide patterns of diversity in a**
2 | **butterfly-**

3 | Balancing selection at a wing pattern locus is associated with major shifts in genome-wide patterns
4 | of diversity and gene flow

5 |

6 | María Ángeles Rodríguez de Cara^{1*\$}, Paul Jay^{1*\$}, Quentin Rougemont^{1*\$}, Mathieu Chouteau^{1,2},
7 | Annabel Whibley^{3,4}, Barbara Huber⁵, Florence Piron-Prunier³, Renato Rogner Ramos⁶, André V. L.
8 | Freitas⁶, Camilo Salazar⁷, Karina Lucas Silva-Brandão⁸, Tatiana Teixeira Torres⁹, Mathieu Joron^{1\$}

9 |

10 | * contributed equally

11 | ¹Centre d'Ecologie Fonctionnelle et Evolutive (CEFE), Univ Montpellier, CNRS, EPHE, IRD,
12 | Montpellier, France

13 | ²Laboratoire Ecologie, Evolution, Interactions Des Systèmes Amazoniens (LEEISA), Université de
14 | Guyane, IFREMER, CNRS, Cayenne, Guyane Française

15 | ³Institut de Systématique Evolution Biodiversité (ISYEB), Museum National d'Histoire Naturelle,
16 | CNRS, Sorbonne-Université, EPHE, Université des Antilles, Paris, France

17 | ⁴School of Biological Sciences, University of Auckland, Auckland, New Zealand

18 | ⁵Instituto de Ciencias Ecológicas y Ambientales (ICAE), Univ de los Andes, Mérida, Venezuela

19 | ⁶Departamento de Biologia Animal, Instituto de Biologia, Unicamp, Campinas, São Paulo, Brazil

20 | ⁷Department of Biology, Faculty of Natural Sciences, Universidad del Rosario, Carrera 24 No 63C-
21 | 69, Bogotá 111221, Colombia.

22 | ⁸Centro de Biologia Molecular e Engenharia Genética, Universidade Estadual de Campinas. Av.
23 | Candido Rondon 400. Campinas, São Paulo, Brazil

24 | ⁹Department of Genetics and Evolutionary Biology, Institute of Biosciences, University of São
25 | Paulo (USP), São Paulo, Brazil

26 | \$ Corresponding authors: angeles.decara@gmail.com, paul.yann.jay@gmail.com,

27 | mathieu.joron@cefe.cnrs.fr, quentinrougemont@orange.fr

28 **Abstract:** Selection shapes genetic diversity around target mutations, yet little is known about how
29 selection on specific loci affects the genetic trajectories of populations, including their genome-
30 wide patterns of diversity and demographic responses. ~~Adaptive introgression provides a way to~~
31 ~~assess how adaptive evolution at one locus impacts whole-genome biology.~~ Here we study the
32 patterns of genetic variation and geographic structure in a neotropical butterfly, *Heliconius numata*,
33 and its closely related allies in the so-called melpomene-silvaniform ~~sub~~clade. *H. numata* is known
34 to have evolved an inversion supergene ~~via the introgression of an adaptive inversion about 2.2~~
35 ~~million years ago, triggering a polymorphism maintained by balancing selection. This locus which~~
36 controls variation in wing patterns involved in mimicry associations with distinct groups of co-
37 mimics, ~~and b~~ Butterflies show disassortative mate preferences and heterozygote advantage at this
38 locus. We contrasted patterns of genetic diversity and structure 1) among extant polymorphic and
39 monomorphic populations of *H. numata*, 2) between *H. numata* and its close relatives, and 3)
40 between ancestral lineages ~~in a phylogenetic framework~~. We show that *H. numata* populations
41 which carry the ~~introgressed~~ inversions as in a balanced polymorphism show markedly distinct
42 patterns of diversity compared to all other taxa. They show the highest genetic diversity and
43 demographic effective population size estimates in the entire clade, as well as a remarkably low
44 level of geographic structure and isolation by distance across the entire Amazon basin. By contrast,
45 monomorphic populations of *H. numata* as well as its sister species and their ancestral lineages all
46 show ~~the lowest~~ effective population sizes and genetic diversity ~~in the clade~~, and higher levels of
47 geographical structure across the continent. ~~This suggests~~ One hypothesis is that the large effective
48 population size of polymorphic populations could be caused by the shift to a regime of balancing
49 selection a property associated with harbouring the supergene due to the genetic load and
50 disassortative preferences associated with inversions. Testing this hypothesis with forward
51 simulations supported the observation of increased diversity in populations with the supergene. Our
52 results are consistent with the hypothesis that the ~~adaptive introgression~~ formation of the ~~inversion~~
53 supergene triggered a ~~shift from directional to balancing selection and~~ a change in gene flow ~~due to~~
54 disassortative mating, causing a general increase in genetic diversity and the homogenisation of
55 genomes at the continental scale.

56
57 **Introduction:** Genetic diversity is shaped by selective processes such as stabilizing or disruptive
58 selection, and by demographic processes such as fluctuations in effective population size. Empirical
59 studies on genetic diversity within and among populations abound, fuelled by an increasing
60 availability of whole genome data, and spurred by our interest in understanding the underlying
61 causes of variation in diversity (e.g. Beichmann 2018, Muers 2009; Murray 2017; Nielsen et al.
62 2009). At the locus scale, strong directional or disruptive selection tends to reduce diversity within
63 populations (Mitchell-Olds et al. 2007), while balancing selection tends to enhance diversity
64 (Charlesworth 2006). Genome-wide factors reducing diversity include low effective population
65 sizes, generating drift, while high genetic diversity is enhanced by large population sizes and gene
66 flow. Overall, it is well recognised that demographic changes should have a genome-wide effect on
67 diversity, while positive selection is expected to play a role on the sites within and around the genes
68 involved in trait variation (Glinka et al. 2003, Muers 2009, Nielsen et al. 2009).

69
70 Variation in behaviour and life-history traits, for instance involving changes in offspring viability or
71 dispersal distance, may also affect species demography, and thus whole genome genetic diversity.
72 However, whether and how genetic variability in a population may be driven by phenotypic
73 evolution at certain traits is poorly understood, and confounding effects may affect patterns of

74 genomic diversity, such as variation in census population size or colonization history. Dissecting
75 how selection on a trait may affect genome-wide diversity can be tackled by comparing closely-
76 related populations differing at this trait coupled with knowledge of when the differences evolved.
77 Here, we took advantage of the dated introgressive origin of a chromosomal inversion associated
78 with major life-history variation to study the demographics and whole genome consequences of
79 changes in the selection regime at a major-effect locus.

80
81 *Heliconius* butterflies are aposematic, chemically-defended butterflies distributed over the
82 American tropics from Southern Brazil to Southern USA (Emsley 1965; Brown 1979) (Fig 1A).
83 *Heliconius* butterflies are well-known for visual resemblance among coexisting species, a
84 relationship called Müllerian mimicry which confers increased protection from bird predators
85 through the evolution of similar warning signals (Sheppard et al. 1985). Most species are locally
86 monomorphic, but their mimicry associations vary among regions, and most species display a
87 geographic mosaic of distinct mimetic “races” through their range. In contrast to most *Heliconius*
88 species, the tiger-patterned *Heliconius numata* is well-known for maintaining both mimicry
89 polymorphism within localities, with up to seven differentiated coexisting forms, and extensive
90 geographic variation in the distribution of wing phenotypes (Brown & Benson 1974; Joron et al.
91 1999). Forms of *H. numata* combine multiple wing characters conveying resemblance to distinct
92 sympatric species in the genus *Melinaea* and other local Ithomiini species (Nymphalidae:
93 Danainae). Polymorphism in *H. numata* is controlled by a supergene, i.e. a group of multiple linked
94 functional loci segregating together as a single Mendelian locus, coordinating the variation of
95 distinct elements of phenotype (Brown & Benson 1974; Joron et al. 2006). Supergene alleles are
96 characterized by rearrangements of the ancestral chromosomal structure, forming three distinct
97 chromosomal forms with zero (ancestral type, Hn0), one (Hn1) or three chromosomal
98 rearrangements (Hn123) (Fig 1B). The ancestral arrangement, Hn0, devoid of inversions, is fixed in
99 most *Heliconius* species (although an inversion in the same region evolved independently in a
100 distantly-related *Heliconius* lineage (Edelman et al. 2019)). Arrangement Hn1 contains a 400kb
101 inversion called P₁ originating from an introgression event about 2.2 My ago from *H. pardalinus*, in
102 which P₁ is fixed (Jay et al. 2018). This introgression is thought to be the founding event triggering
103 the formation of the supergene and the maintenance of polymorphism in *H. numata* (Jay et al.
104 2018). Arrangement Hn123 displays two additional inversions, P₂ and P₃, in linkage with P₁, and
105 therefore originated after the introgression of P₁ into the *H. numata* lineage (Jay et al. 2021).

106
107 *Heliconius numata* is widespread in the lowland and foothill tropical forests of the Amazon basin,
108 the Guianas, and the Brazilian Atlantic Forest (Mata Atlântica), but the frequencies of the three
109 chromosome arrangements vary across the range. Ancestral type Hn0 is fixed in the Atlantic Forest
110 populations of Brazil (forms *robigus* or *ethra*), but segregates at intermediate frequencies in all
111 other *H. numata* populations throughout the range (forms *silvana* and *laura*) (Fig 1C). Chromosome
112 type Hn1 is associated with the Andean mimetic form *bicoloratus* and is found in the Eastern
113 Andean foothills of Ecuador, Peru, and Bolivia. Chromosome type Hn123 is associated with a large
114 diversity of wing-pattern forms of intermediate allelic dominance, including *tarapotensis*, *arcuella*
115 and *aurora*, and is reported from Andean, lowland Amazonian and Guianese populations. Inversion
116 polymorphism is therefore structured across the range, with populations being fixed for the
117 ancestral chromosome (Atlantic Forest, see Text S1 & Table S1-2), or displaying a polymorphism
118 with two (Amazon-Guiana) or three (Andes) chromosomal types in coexistence (Joron et al. 2011).
119 Monomorphic populations of the Atlantic forest, devoid of rearrangements at the supergene locus,

120 might represent the ancestral state displayed by *H. numata* populations before the evolution of the
121 supergene via introgression (Fig 1C).

122

123 The wing patterns of *H. numata* are subject to selection on their resemblance to local co-mimics
124 (Chouteau et al. 2016), but the polymorphism is maintained by balancing selection on the
125 chromosome types. Balancing selection is indeed mediated by disassortative mating favouring
126 mixed-form mating (Chouteau et al. 2017) and is likely to have evolved in the response to the
127 deleterious mutational load carried by inversions, which causes heterozygous advantage in *H.*
128 *numata* (Jay et al. 2021, Faria et al. 2019, Maisonneuve et al. 2019). The introgression of P₁ and the
129 formation of a supergene were associated with a major shift in the selection regime (Jay et al.
130 2018). ~~and in the~~ The mating system was also changed during or after introgression. These events and
131 may therefore have profoundly affected the population biology of the recipient species, *H. numata*.
132 We investigate here whether the adaptive introgression of a balanced inversion is associated with a
133 signature in the genetic diversity and geographic structure. In particular, we predict that genetic
134 diversity should be higher in *H. numata* than in closely related taxa. Similarly nucleotide diversity
135 should be higher in all polymorphic populations carrying either one segment (Hn1) or two
136 (Hn1,Hn123) compared to the population that is monomorphic and only carries ~~only~~ the non-
137 inverted segment (Hn0) in the Brazilian Atlantic Forest. We analyse changes in the demographic
138 history of the clade containing *H. numata* and closely related taxa, as well as their current patterns
139 of diversity and demography, using three well separated populations of *H. numata* representing
140 different states of inversion polymorphism. ~~Our results are consistent with the selection regime and~~
141 ~~mating system associated with supergene formation having enhanced gene flow among populations~~
142 ~~and increased effective population size. Our results suggest that following supergene formation, a~~
143 ~~change in the selection regime and mating system may have facilitated gene flow among morphs~~
144 ~~and had key consequences in current patterns of genetic structure. Moreover, our findings highlight~~
145 ~~that balancing selection and a shift in mating systems associated with chromosomal polymorphism~~
146 ~~may reshape genomewide diversity, with crucial consequences on current patterns of genetic~~
147 ~~structure and population ecology.~~

148

149 **Material and Methods**

150 We used here whole genome resequencing from 137 specimens of *Heliconius*, including 68 *H.*
151 *numata*. Sampling included specimens from populations in the Andean foothills (3 chromosome
152 types), from the upper Amazon (2 chromosome types), from French Guiana (2 chromosome types)
153 and from the Brazilian Atlantic Forests (1 chromosome type) (Fig 1C; Table S3). Related taxa were
154 represented by the sister species *H. ismenius*, found west of the Andes (parapatric to *H. numata*), by
155 Amazonian representatives of the lineage *H. pardalinus* (donor of the inversion), *H. elevatus*, *H.*
156 *ethilla*, *H. besckei* as well as *H. hecale*, and by *H. melpomene* and *H. cydno* as outgroups. Only
157 Andean, Amazonian and Guianese populations of *H. numata* display chromosomal polymorphism,
158 all other taxa being fixed for the standard gene arrangement (Hn0), or for the inverted arrangement
159 Hn1 (*H. pardalinus*) (Jay et al. 2018). Hereafter, *H. numata* populations from the Andes, Amazon
160 and French Guiana will be collectively referred to as “Amazonian”, and populations from the
161 Atlantic Forest as “Atlantic”. Butterfly bodies were preserved in NaCl saturated DMSO solution at
162 20°C and DNA was extracted using QIAGEN DNeasy blood and tissue kits according to the
163 manufacturer’s instructions with RNase treatment. Illumina Truseq paired-end whole genome
164 libraries were prepared and 2x100bp reads were sequenced on the Illumina HiSeq 2000 platform.
165 Reads were mapped to the *H. melpomene* Hmel2 reference genome (Davey et al., 2016) using

166 Stampy (version 1.0.28; Lunter and Goodson, 2011) with default settings except for the substitution
167 rate which was set to 0.05 to allow for the expected divergence from the reference of individuals in
168 the so-called silvaniform clade (*H. numata*, *H. pardalinus*, *H. elevatus*, *H. hecale*, *H. ismenius*, *H.*
169 *besckei* and *H. ethilla*). *H. melpomene* and *H. cydno* belonging to the so-called *melpomene* clade,
170 their genomes were mapped with a substitution rate of 0.02. Alignment file manipulations were
171 performed using SAMtools v0.1.3 (Li et al. 2009). After mapping, duplicate reads were excluded
172 using the *MarkDuplicates* tool in Picard (v1.1125; <http://broadinstitute.github.io/picard>) and local
173 indel realignment using IndelRealigner was performed with GATK (v3.5; DePristo et al. 2011).
174 Invariant and polymorphic sites were called with GATK HaplotypeCaller, with options --
175 min_base_quality_score 25 --min_mapping_quality_score 25 -stand_emit_conf 20 --heterozygosity
176 0.015.

177
178 F_{ST} , d_{XY} and π , were calculated in overlapping windows of 25 kb based on linkage disequilibrium
179 decay (*Heliconius* Genome Consortium 2012) using custom scripts provided by Simon H. Martin
180 (<https://github.com/simonhmartin>), and the genome-wide average was calculated using our own
181 scripts (available from <https://github.com/angelesdecarra>). Distance in km between sampling sites
182 was measured along a straight line, not taking into account potential physical barriers. Following
183 Rousset (1997), in a 2-dimensional habitat, under a model of isolation by distance (IBD)
184 differentiation, measured as $F_{ST}/(1-F_{ST})$, should increase as a function of the logarithm of the
185 distance. Therefore, we tested for the existence and intensity of an IBD signal among species and
186 between populations of *H. numata* using a linear model. If IBD is stronger in species not
187 polymorphic for the inversion we should observed significantly steeper slopes in these species. To
188 test this, we measured IBD (i) within populations of each species separately, (ii) for all *H. numata*
189 within the Amazonian forestregion but without-(excluding the-Atlantic forest populations) and (iii)
190 for all *H. numata* including the Atlantic region. The slopes of $F_{ST}/(1-F_{ST})$ versus $\log(\text{distance})$ were
191 calculated using the R package *lsmeans* (Lenth 2016); the slope difference among species or
192 between populations within species was estimated with an ANOVA and its significance evaluated
193 with function pairs of this package (Text S1 and see example script on github.com/angelesdecarra/).

194
195 Admixture (Alexander et al. 2009) analyses were run on a subset of the 68 *H. numata* genomes,
196 keeping only 15 individuals from Peru to have a more balanced representation of individuals across
197 the geographic distribution. Filters were applied to keep biallelic sites with minimum mean depth
198 of 8, maximum mean depth of 200 and at most 50% genotypes missing. We only kept 1 SNP per
199 kilobase to remove linked variants using the thinning function in vcfutils, and we obtained the
200 optimal number of clusters using cross-validation for values of K from 1 to 10 (Alexander et Lange,
201 2011a, 2009). Principal component analyses (PCA) were performed with the same filters as for
202 admixture, using the same *H. numata* genomes as for the admixture analyses, using ~~smartpca~~
203 (Patterson et al. 2006) plink2 (Chang et al. 2015).

204
205 In order to estimate demographic parameters independently of the effect of selection on diversity,
206 we performed stringent filtering on the dataset. We removed all predicted genes and their 10,000
207 base-pair flanking regions, before performing G-PhoCS (Gronau et al. 2011) analyses as detailed
208 below. Repetitive regions were masked using RepeatMasker and Tandem Repeat Finder (Benson
209 1999). GC islands detected with CpGcluster.pl with parameters 50 and 1E-5 (Hackenberg et al.,
210 2006) were also masked. Scaffolds carrying the supergene rearrangements (Hmel215006 to
211 Hmel215028) were excluded, as were scaffolds from the sex chromosome (Z) and mtDNA, since

212 those are expected to show unusual patterns of diversity due to selection and different effective
213 population sizes.

214

215 We analysed the demographic history of *H. cydno*, *H. numata*, *H. ismenius*, *H. pardalinus* and *H.*
216 *elevatus* with G-PhoCS, which allows for the joint inference of divergence time, effective
217 population sizes and gene flow. In order to detect differences in demography correlating with the
218 presence of the supergene in *H. numata*, we conducted analyses separating the Atlantic population
219 of *H. numata* from Amazonian populations. G-PhoCS is an inference method based on a full
220 coalescent isolation-with-migration model. Inferences are conditioned on a given population
221 phylogeny (based on Kozak et al. 2015) with migration bands (i.e. priors in the migration rates) that
222 describe allowed scenarios of post-divergence gene flow. The model assumes distinct migration rate
223 parameters associated with each pair of populations, and allows for asymmetric gene flow. Given
224 the computational burden of G-PhoCS, we selected two individuals per taxon or population,
225 retaining those with the highest sequencing depth (see Table S3). The input dataset consisted of
226 4092 genomic regions, each 1kb in length and spaced at approximately 30kb intervals (above the
227 value at which LD decay at more than half of its value) and with genotypes in at least one of the
228 two samples of each taxon We used as priors for coalescence times (τ) and genetic diversity (θ),
229 Gamma functions with $\alpha=1$ and $\beta=100$, and for migration bands rates $\alpha=0.002$ and $\beta=0.00001$.
230 These priors were chosen to allow good convergence while also ensuring non informativity. In
231 order to calculate the highest posterior density interval, we used the library HDInterval in R, and to
232 integrate such posterior densities we used the library sfsmisc in R. We rescaled the results using a
233 mutation rate of $1.9E-9$ (Martin et al. 2016) and 4 generations per year (i.e., $g=0.25$). Migration
234 bands were considered significant following the criteria of Freedman et al. (2012): if the 95% HPD
235 interval did not include 0 or if the total migration rate (migration rate times the duration of the
236 migration band) was larger than 0.03 with posterior probability larger than 0.5.

237

238 **Demographic Reconstruction of population size changes, split and mixtures**

239 The G-phocs method provided useful information across all species but i) do not allow to quantify
240 the time scale of population size change, ii) is limited in the number of individuals it can handle and
241 iii) displayed limited accuracy to distinguish N_e and m in a simulation study (Gronau et al. 2011).
242 We thus constructed additional models to test the hypothesis that *H. numata* populations with
243 inversion polymorphism display an increased effective population size due to disassortative mating
244 To test this, we used $\partial a \partial i$ to reconstruct the demographic history of *H. numata* individuals from the
245 Amazonian forest, quantify their historical changes in effective population size and test their
246 divergence history from 1) *H. numata* from the Brazilian area, which do not carry the inversion; and
247 2) *H. pardalinus* individuals. We allowed for change in effective population size in both the
248 ancestral populations. Theoretically, the change in effective population size in *H. numata* associated
249 with the change in mating system should be more recent than the time of introgression of the
250 inversion into *H. numata*. To verify this hypothesis we allowed for change in N_e of the daughter
251 population at any time after the split. We tested different models of divergence with and without
252 (asymmetric) migration and included the effect of linked selection (e.g. Roux et al. 2016).

253 Since, the conditions of historical divergence are not known, we tested a model of divergence with
254 ongoing migration (IM) a model of divergence with ancient migration if gene-flow has stopped
255 recently (AM) and, in the case of divergence into multiple refugia, a model of secondary contact
256 (SC). We also included a model of Strict Isolation (SI) as a null model.

257 The models shared the following parameters: the ancestral populations of size N_{anc} can grow or
258 shrink to a size N_{anc2} between T_{anc} and up until its splits at time T_{split} into two daughter populations of
259 size N_1 and N_2 . Under the SI model, no gene flow occurs between the two populations. Under AM,

260 gene flow occurred between T_{split} and T_{am} and is followed by a period of strict isolation. Under IM,
261 gene flow occurs at a constant rate at each generation between the two populations. Gene flow can
262 be asymmetric, so that two independent migration rates m_{12} (from population 2 to 1) and m_{21} (from
263 population 1 to 2) were modeled. Under the SC model, the population evolved in strict isolation
264 between T_{split} and until T_{sc} where a secondary contact occurs continuously up to present time. Gene
265 flow is modeled as $M = 2N_{REF}m$. In $\partial a\partial i$, heterogeneity in effective population size was used to
266 account for linked selection by defining two categories of loci with varying effective population
267 sizes (proportion $1-Q$ of loci with a “neutral N_e ” and a proportion Q of loci with a reduced effective
268 population size due to either selection at linked site). To quantify how linked selection affects
269 reduced N_e , we used a Hill-Robertson scaling factor (Hrf) to relate the effective population size of
270 loci influenced by selection ($N_r = Hrf * N_e$) to that of neutral loci (N_e). A hierarchical approach was
271 used to avoid over-fitting: first we compared models assuming constant effective population size.
272 Second, the best identified models were modified to incorporate population expansion or decline, as
273 expected given the observed distribution of genetic diversity. Population expansion was
274 implemented using two additional parameters for population 1 and population 2, allowing each
275 population to either grow or decline exponentially at any time after their split from the ancestral
276 population (controlled by parameters s_1 and s_2 for population 1 and 2 respectively).
277 Models were fitted using the diffusion theory implemented in $\partial a\partial i$ (Gutenkunst et al. 2009) and
278 includes the effect of linked selection. $\partial a\partial i$ uses the SFS as a summary of the data. For a given
279 demographic model, the SFS is computed using diffusion approximation and compared to the
280 empirical SFS using AIC.
281 We used stringent filtering ($GQ > 30$, $4 < \text{mean depth} < 80$) and no missing data to keep high
282 quality sites and remove potential paralogs or PCR duplicates exhibiting excessive read depth. To
283 minimize linkage we subset our data to keep one SNP every 5kb. No MAF filter was used and
284 singletons were kept to avoid ascertainment bias in estimates of demographic parameters. For each
285 model, 32 independent replicate runs were performed and only models with the lowest AIC and
286 ΔAIC were kept.

288 **Forward Simulations**

289 In order to better understand the nature of the processes that generate higher genetic diversity in *H.*
290 *numata* compared to closely related taxa, we used simulations to test the hypothesis that
291 disassortative mating generates an increase in levels of genetic diversity at a genome-wide scale.
292 We hypothesized that such level of genetic diversity is higher than expected under i) random mating
293 (a model similar to panmixia) or ii) assortative mating, as commonly observed in other *Heliconius*
294 species. To test this hypothesis we run forward simulation under disassortative, assortative and
295 random mating using slim v3.6 (Messer et al. 2013).
296 We simulated a stepping stone model with 10 demes, each composed of 1,000 diploid individuals
297 and connected by a (symmetric) migration parameter (m). Each individual received neutral and
298 deleterious (ratio 16:6) mutations at a rate $\mu = 1e-8$ μ /bp/generation (rescaled to $\mu = 1e-6$ for faster
299 simulation of a larger population). We simulated an individual with a pair of 1Mb chromosome,
300 including a single locus with 5 alleles with perfect dominance (allele 1 > allele 2 > allele 3 > allele
301 4 > allele 5) given 5 possible alternative phenotypes (referred hereafter as “morph”). Each allele
302 was fully linked (no recombination) with a given deleterious recessive mutation, generating
303 overdominance at this loci so that polymorphism is always maintained. Local adaptation was
304 introduced in the model through a single parameter defining randomly which morphs were favored
305 in each population. In each population, either 2 or 3 morphs benefited from a fitness advantage
306 compared to the others. The fitness reduction varied between 0 (= fitness of zero for migrants in a
307 demes) and 1 (no reduction of fitness). We tested 3 possible values for this parameter (0, 0.25 and
308 0.5).

309 Finally, disassortative mating was controlled by a mate choice parameter defining whether a morph
310 would reproduce with another morph. The strength of the parameter varied between 0 (= complete
311 disassortative mating) and 1 (= no mating weight). We tested 3 possible values for this parameter
312 (0, 0.25 and 0.5).
313 We run the model for 80,000 generations to reach demographic equilibrium and assessed levels of
314 synonymous diversity (π_s). We tested all combinations of the 3 values for levels of disassortative
315 mating and local adaptation and ran 10 replicates per combination in order to estimate the variance
316 around π_s .
317 Similarly, we run a model with strict assortative mating, controlled by a parameter defining whether
318 similar morphs reproduced together. The strength of the parameter varied between 0 (complete
319 assortative mating where a given individual mate only with an identical morph) and 1 (where
320 individual mate randomly with regards to the morph). We tested 3 possible values for this parameter
321 (0, 0.25 and 0.5). As for disassortative mating, all combinations of assortative mating and local
322 adaptation values were tested. For each model we tested 3 values for the migration rate, $m = 1e-4,$
323 $1e-6$ and $1e-8$, resulting in a total of 54 comparisons.
324 For graphical display in Figure 4, the values of assortative/disassortative mating were rescaled on a
325 scale between (0 and 1) with 0 indicating no disassortative mating but complete assortative mating
326 and 1 complete disassortative mating (or no assortative mating). A value of 0.5 was equivalent to
327 random mating.

328

329 **Results**

330 Using cross validation error as a measure of the optimal number of clusters with Admixture, we
331 found that $K=2$ was the optimal cluster number describing within-species genetic variation in *H.*
332 *numata* (Fig 2A). One cluster corresponds to the Atlantic population, forming a well-differentiated
333 genetic entity compared to all other *H. numata* populations. All Amazonian populations of *H.*
334 *numata* showed a remarkable uniformity, ~~with the exception of a few individuals sharing some~~
335 ~~variation with SE Brazil.~~ This pattern is consistent with the population structure inferred using
336 microsatellite markers (Fig S1). Population structure revealed by PCA is in line with the admixture
337 analysis (Fig 2B). ~~Individuals from the Atlantic populations of *H. numata* clustered together to one~~
338 ~~side of the first PCA axis, whereas all other individuals from all other populations clustered to the~~
339 ~~other side. The second axis of the PCA separates individuals from French Guiana from the other~~
340 ~~samples of the upper Amazon. This clustering separation was not found with Admixture (i.e. with~~
341 ~~$K=3$) from the complete dataset. To better investigate the existence of a hierarchical population~~
342 ~~structure, we excluded individuals from the Atlantic populations and compared individuals from~~
343 ~~French Guiana to a randomly sampled set of Peruvian individuals. In this case we found a clear~~
344 ~~separation in two groups corresponding to French Guiana and Peru (Fig S2A). The same pattern~~
345 ~~was observed when replacing Peru by Colombia or Ecuador (Fig S2B,C), suggesting that the~~
346 ~~divergence between Amazonian populations is very reduced.~~ In accordance, pairwise genome-wide
347 estimates of differentiation (F_{ST}) between *H. numata* populations showed elevated values when
348 comparing the Atlantic population to other populations, low values between French Guiana and
349 other Amazonian population, and were the lower but very small values when comparing pairs of
350 Amazonian populations outside of French Guiana, even at a large distance (Fig 2C, Table S4). For
351 instance, the population from La Merced in Peru shows an $F_{ST} = 0.032$ with the population from
352 French Guiana at a distance of 3019km, but an $F_{ST} = 0.311$ (an order of magnitude higher) with the
353 Atlantic population at a similar distance. The comparison between La Merced and Ecuador was
354 even lower ($F_{ST} = 0.0159$). Isolation by distance among Amazonian populations of *H. numata*,

355 estimated using the proxy $F_{ST}/1-F_{ST} \sim \log_{10}(\text{km})$ was significant ($R^2 = 0.41$, $p = 1.61e-06$, slope =
356 ± 0.02). Comparison among other species did not revealed any significant IBD ($R^2 = 0.01$, $p = 0.29$,
357 slope = 0.12). shows a very different pattern to other species, with a highly significantly shall. An
358 analysis of the slope revealed a lower rate of increase in F_{ST} with distance in *H. numata* compared to
359 all other taxa (Fig 2C, Table S4, Supp Text S1). By contrast, differentiation as a function of
360 distance IBD between Atlantic and Amazonian populations of *H. numata* is close to what is
361 observed in other species, and not significantly different (see Supp. Text S1).

363 Analyses of genetic diversity show that all populations of *H. numata*, except those from the Atlantic
364 Forest, have a similarly high genetic diversity (Fig 3A). By comparison contrast, closely related
365 *Heliconius* taxa show significantly lower genetic diversity (Fig 3A). These patterns are similar to
366 those obtained using G-PhoCS to analyse the demographic histories in a phylogenetic context,
367 where Amazonian populations of *H. numata* show higher population sizes compared to the Atlantic
368 populations (Fig 3B, Table S5). G-PhoCS analyses also show a demographic history in which gene
369 flow plays a crucial role (Table S6). For instance, our analyses show strong significant gene flow
370 right at the beginning of the divergence between *H. ismenius* and the other silvaniforms, as well as
371 in the divergence between *H. pardalinus* and *H. elevatus*. The effective population sizes inferred
372 from Atlantic genomes are one order of magnitude lower than that those obtained using *H. numata*
373 populations from other localities (Fig 3A and Table S5). In our cladogram, the increase in *H.*
374 *numata* population size is restricted to the Amazonian branch, excluding Atlantic populations.

376 **Demographic reconstruction from *daði***

377 The model selection procedure based on AIC gave higher support for a model of secondary contact
378 (SC) in the pairwise comparison between *H. numata* from Peru and *H. numata* from Brazil. The
379 pairwise comparison between *H. numata* and *H. pardalinus* supported a model of divergence with
380 continuous gene-flow (IM) (Table S7, Figure S3). All models supported an expansion occurring in
381 the ancestral population, followed by further growth of the *H. numata* carrying the inversion
382 supergene to reach a size of several millions, which was by far the largest effective size compared
383 to all other species. This stands in stark contrast with the results observed in the samples from
384 Brazil (which do not harbor the inversion) (Table 2). Accordingly, *H. numata* populations from the
385 Atlantic forests of Brazil appear to have been subject to a bottleneck at the start of their divergence
386 from Amazonian populations, followed by exponential growth, suggesting a strong (and recent)
387 founding event, leading to a comparatively smaller population size than that observed in the rest of
388 *H. numata*. It is worth noting however that effective population size was hard to estimate in
389 pairwise comparisons between *H. numata* from Peru and SE Brazil. Indeed, parameter uncertainty
390 was large, and model residuals (Figure S3) were also large. Our results indicated that *H. pardalinus*
391 displayed an initially large population size followed by a comparatively smaller size expansion than
392 *H. numata* (Table 2). Estimates of current effective population sizes are therefore qualitatively
393 similar to those from G-phocs.

395 **Forward simulations**

396 Forward simulations under different levels of local adaptation (controlled by the strength of
397 divergent selection), disassortative mating and migration are displayed in Figure 4B. The same
398 results under a model of assortative mating involving different levels of selection and migration are
399 displayed in Figure 4A. Overall, synonymous genome-wide nucleotide diversity (π_S) was higher in
400 73 % of the models including disassortative mating (average $\pi_S = 0.0145$) when compared to their

401 equivalent under assortative mating (average $\pi_S = 0.011$), a weak but significant difference (p
402 <0.01 , see Figure S5). In summary, modest differences were observed among models with different
403 strengths of divergent selection or disassortative mating, the most influential variable being the rate
404 of migration (Figure 4).

405

406 Discussion

407 Our results suggest that populations displaying inversion polymorphism in the *P* supergene in *H.*
408 *numata* also display distinctive population demography and gene flow. Differences in demographic
409 and differentiation regimes associated with structural variation at this locus are revealed when
410 comparing polymorphic populations of *H. numata* to closely-related monomorphic taxa, such as (1)
411 peripheral populations of *H. numata*, (2) sister taxa, and (3) inferred ancestral lineages. This
412 suggests that the existence of a mimicry supergene controlling polymorphism in *H. numata* is may
413 be associated, in time and in space, with major differences in population biology. We hypothesize
414 this to be due to a change in the balancing selection regime due to heterozygote advantage (Jay et
415 al. 2021) and in the associated evolution of disassortative mating (Chouteau et al. 2017) following
416 the onset of inversion polymorphism, causing direct effects on ecological parameters such as gene
417 flow, immigration success and effective population size. Testing this hypothesis through forward
418 simulation yielded mixed evidence for a genome-wide effect of this disassortative mating,
419 especially when compared to a simple model of random mating.

420

421 Our analyses show large-scale variation in genetic diversity among closely related taxa in this clade
422 of *Heliconius* butterflies. Within *H. numata*, the genetic diversity of found in polymorphic
423 Amazonian populations is ~4 times one to two orders of magnitude higher than the diversity found
424 in populations from the Atlantic Forest. Generally, Amazonian populations of *H. numata* harbour
425 the highest genetic diversity in the entire *melpomene/silvaniform* clade, which contrasts with the
426 low diversity found in the most closely related taxa such as *H. ismenius* or *H. besckei*. Inferring
427 historical demography during the diversification of the *H. numata* lineage reveals that the large
428 effective population size in that species is only associated with the branch representing
429 polymorphic, Amazonian *H. numata* populations, while internal branches all show very low
430 diversity estimates. This suggests that ancestral and putatively monomorphic populations of *H.*
431 *numata* were similar in their diversity parameters to current sister species *H. ismenius* populations,
432 or to current peripheral Atlantic *H. numata* populations. Although low-diversity lineages could have
433 lost diversity due to recent events such as strong bottlenecks, the distribution of parameters across
434 as estimates of effective population size lineages rather from dadi indicated for the Atlantic
435 population. suggests Nevertheless our dadi estimates do suggest that the Amazonian populations of
436 *H. numata* underwent a dramatic increase in effective population size posterior to their split with
437 Central American (*H. ismenius*), *H. pardalinus* and the Atlantic populations. Those findings are in
438 agreement with G-Phocs analyses. The Amazonian branch of the *H. numata* radiation is
439 characterized by the long-term maintenance of inversion polymorphism, triggered by the
440 introgression of a chromosomal inversion about 2.2 Ma ago. Therefore, the major shift in
441 demography between Amazonian and Atlantic populations indeed appears associated to coincide,
442 at least in the broad sense, with the occurrence of inversion polymorphism, even though the lack of
443 replication of this event impedes firmly establishing causality here.

444

445 Another striking result is the low-lack of genetic structure displayed by *H. numata* across the
446 Amazon, with all Amazonian and Guianese populations forming a single genetic cluster. Only

447 Atlantic populations stand out and display high differentiation with other *H. numata* from the rest of
448 the range. French Guiana and Peruvian populations, separated by over 3000 km across the
449 Amazon, are ~~remarkably genetically~~ weakly genetically differentiated ~~similar~~ compared to pairs of
450 populations at comparable distances in other species, and show only modestly stronger ~~similar~~
451 differentiation than pairs of *H. numata* populations taken at short distances. *H. numata*
452 populations from the Amazon show significantly lower isolation by distance than all other taxa, as
453 measured by the change in F_{ST} across distance (F_{ST}/km) (Fig. 2C), with a very distinctive, flat slope
454 of isolation by distance. The only exception is found when comparing Amazonian populations with
455 Atlantic populations of Brazil, displaying a level of differentiation in line with that of pairs of
456 populations at similar distances within other taxa.

457

458 Effective population size is affected by census size, mating system, and the force and type of
459 selection acting on traits (Charlesworth 2009). Selection is often viewed as a force only affecting
460 the genetic variation around specific, functional loci in the genome, but it may also affect whole
461 genome diversity, for instance when its action is sufficient to modify local demography or mating
462 patterns. In *H. numata*, morphs and therefore inversion genotypes show disassortative mate
463 preferences, i.e., they preferentially mate with individuals carrying different chromosome types
464 (Chouteau et al. 2017). Disassortative mating enhances heterozygosity and the mating success of
465 individuals expressing rare alleles (negative frequency dependence) (Knoppien 1985; Hedrick et al.
466 2018). Consequently, immigrants expressing rare, recessive alleles have a mating advantage in *H.*
467 *numata*. Disassortative mating associated with the supergene should therefore bring an advantage to
468 immigrant genomes in LD with recessive supergene alleles, possibly enhancing genome-wide gene
469 flow. ~~Supergenes are also characterised by monosingle-locus Mendelian inheritance, by which~~
470 ~~mimicry phenotypes are maintained in the face of recombination, even after immigration. This~~
471 ~~Effective migration regime~~ ~~regime in populations harbouring a mimicry supergene is therefore~~
472 likely to be quite different to that observed in other mimetic taxa such as *Heliconius melpomene* or
473 *H. erato*, in which mimicry variation is controlled by multiple loci with diverse dominance patterns.
474 In those taxa, hybrid offspring display recombinant patterns breaking down mimicry, even after
475 multiple generations of backcrossing, and pure forms mate assortatively with respect to wing
476 pattern (McMillan et al. 1997, Mallet et al. 1998, Jiggins et al. 2001); both processes select against
477 mimetic variants migrating from adjacent areas with distinct warning patterns. ~~The expectation is~~
478 that immigrant genomes should be consistently associated with mimicry breakdown in the case of
479 multilocus architectures, which should translate into an effect on effective migration genomewide,
480 compared to situations with polymorphic mimicry supergenes. In *H. numata*, the evolution of a
481 polymorphic mimicry supergene and disassortative mate preferences could therefore explain the
482 relative lack, compared to other *Heliconius* taxa, of differentiation among polymorphic populations,
483 even across large distances. Furthermore, enhanced gene flow could also cause an increase in
484 effective population size estimates (Slatkin 1987), putatively explaining why polymorphic
485 populations of *H. numata* harbour the highest genetic diversity, and display the highest N_e estimates
486 in the entire *melpomene-silvaniform* clade of *Heliconius*. These hypotheses are also supported by
487 our forward simulation which suggests that indeed, disassortative mating resulted in enhanced
488 genetic diversity compared with assortative mating, although the effect was small. In addition, our
489 results also suggests that a simple model of random mating may explain well the data, thus purely
490 demographic expansions may also generate high genetic diversity and high effective population
491 size, as observed from our $\partial a \partial i$ demographic modelling.

492

493 Alternative processes may of course contribute to the observed patterns. Amazonian and Atlantic
494 populations may differ in other aspects that could also result in differences in genetic diversity.
495 Habitat availability and structure may be different, possibly entailing differences in the maintenance
496 of diversity. The Atlantic Forest is vast in area, but may represent a smaller biome compared to the
497 Amazon, and is isolated from the bulk of the range of *H. numata*, which could result in a
498 populations ~~ecology~~ displaying characteristics of peripheral populations with smaller effective
499 population sizes (Eckert et al. 2008). Reduced effective population size is supported by our data.
500 One major caveat associated to our inference remains the small number of individuals (n = 12) from
501 the Atlantic forest. Genetic ~~diversity~~ might be underestimated, notably if populations have a history
502 of fragmentation in this area. The other *Heliconius* species in the clade have much in common with
503 *H. numata* in terms of habitat and general ecology, yet their niche and life-history specificities and
504 their phylogenetic histories may result in consistent differences with the polymorphic *H. numata*
505 populations. All those specificities may contribute to the observed pattern in which polymorphic
506 Amazonian populations of *H. numata* display high effective population size and a ~~lack of weak~~
507 geographic structure in genome-wide genetic variation. Yet this pattern of variation correlates
508 parsimoniously with the evolution of a supergene causing disassortative mating and single-locus
509 control of mimicry variation in certain Amazonian *H. numata* populations, which provides an
510 elegant mechanism explaining their differences with extant and ancestral closely-related lineages.
511 However, we cannot rule out a role for conjectural differences in ecology and geography with all
512 other taxa.

513

514 In conclusion, our results show a remarkable contrast in the demography and differentiation of
515 populations within the Amazonian range of *H. numata* compared to closely related taxa and
516 ancestral lineages, as well as with other taxa in the *melpomene*/silvaniform clade. ~~Although those~~
517 ~~populations may differ in many uncharacterized ways from all other taxa, one known and consistent~~
518 ~~difference is the maintenance of inversion polymorphism associated with a specific mating system~~
519 ~~and selection regime in Amazonian *H. numata*.~~ ~~Theis~~ distinctiveness of the ~~onlyis~~ widely
520 polymorphic ~~populations species~~ in the clade is consistent with the hypothesis that the evolution of
521 a supergene maintained by balancing selection represents a major transition in this lineage,
522 triggering changes in genome-wide patterns of diversity and population ecology over the last 2
523 million years since its formation. If this hypothesis is correct, the evolution of a locus under
524 balancing selection may therefore feed-back on population ecology and diversification, and
525 consequently on speciation.

526

527 Eco-evolutionary feedbacks between changes in genomic architecture and the ecological parameters
528 of populations are still not well understood and few cases have been studied. The evolution of self-
529 incompatibility ~~in~~ in plants, affecting the rules of mating and feeding back on population ecology,
530 connectivity, and demography, may be one example, but effects of the evolution of trait genetic
531 architecture on population ecology may be more common than previously thought. In our study,
532 more work on the determinants of variation in effective population sizes in the genus *Heliconius* is
533 needed to determine the precise impact of the supergene on demography in *H. numata*.

534 ~~More work on the determinants of variation in effective population sizes in the *Heliconius* genus is~~
535 ~~needed to determine the precise impact of the supergene on demography of *H. numata*.~~ We believe
536 that our results emphasize a potential link between genomic architecture, selection and demography,
537 and should inspire future theoretical and modelling studies. ~~Finally, the eco-evolutionary feedbacks~~
538 ~~between changes in genomic architecture and the ecological parameters of populations are well-~~

539 | ~~known when considering self-incompatibility loci in plants, but may be more common than~~
540 | ~~previously thought.~~ Indeed, Overall our result suggests that balancing selection maintaining
541 | structural polymorphisms affecting life-history traits may have a profound influence on species
542 | ecology.
543

544 **Contributions:**

545 | MARdC, PJ, QR and MJ designed the study and wrote the manuscript. BH, AVLF, TTT, RRR,
546 | KLSB provided the Atlantic samples. CS provided the Colombian samples. MARdC, ~~and~~ PJ and
547 | QR performed genomic analyses and simulations with input from AW. MARdC, PJ, MJ, FPP and
548 | MC collected the Peruvian and Ecuadorian samples. MC performed microsatellite analyses and
549 | organized fieldworks and butterfly rearing. All authors contributed to editing the manuscript.

550 **Aknowledgements:**

551 | This work was funded by grants ~~HYBEVOL-Hybevol~~ (ANR-12-JSV7-0005) and Supergene (ANR-
552 | 18-CE02-0019-01) from the Agence Nationale de la Recherche and European Research Council
553 | Grant MimEvol (StG-243179). We acknowledge the Genotoul and the Montpellier Bioinformatics
554 | Biodiversity (MBB) platforms for providing us with calculation time. We thank Dr. Vitor Becker, at
555 | the Serra Bonita Reserve (Bahia), Alexandre Soares, at the MN/UFRJ (Rio de Janeiro) and Dr.
556 | Marcelo Duarte at the MZ/USP (Sao Paulo) for their contribution to the collection of butterflies in
557 | Brazil. Field collections in Colombia were conducted under permit no. 530 issued by the Autoridad
558 | Nacional de Licencias Ambientales (ANLA). We are grateful to Marianne Elias and Violaine
559 | Llaurens, ~~Quentin Rougemont~~ for comments and discussions. AVLF acknowledges support from
560 | Fundação de Amparo à Pesquisa do Estado de São Paulo – (FAPESP) (Biota-Fapesp grants
561 | 2011/50225-3, 2013/50297-0) and Conselho Nacional de Desenvolvimento Científico e
562 | Tecnológico (CNPq) (421248/2017-3 and 304291/2020-0). KLSB acknowledges the financial
563 | support of FAPESP Process # 2012/16266-7. Brazilian specimens are registered under SISGEN
564 | (A701768).
565

566 **Data availability:**

567 | The raw sequence data were deposited in NCBI SRA and accession numbers are indicated in
568 | Supplementary table 3.
569

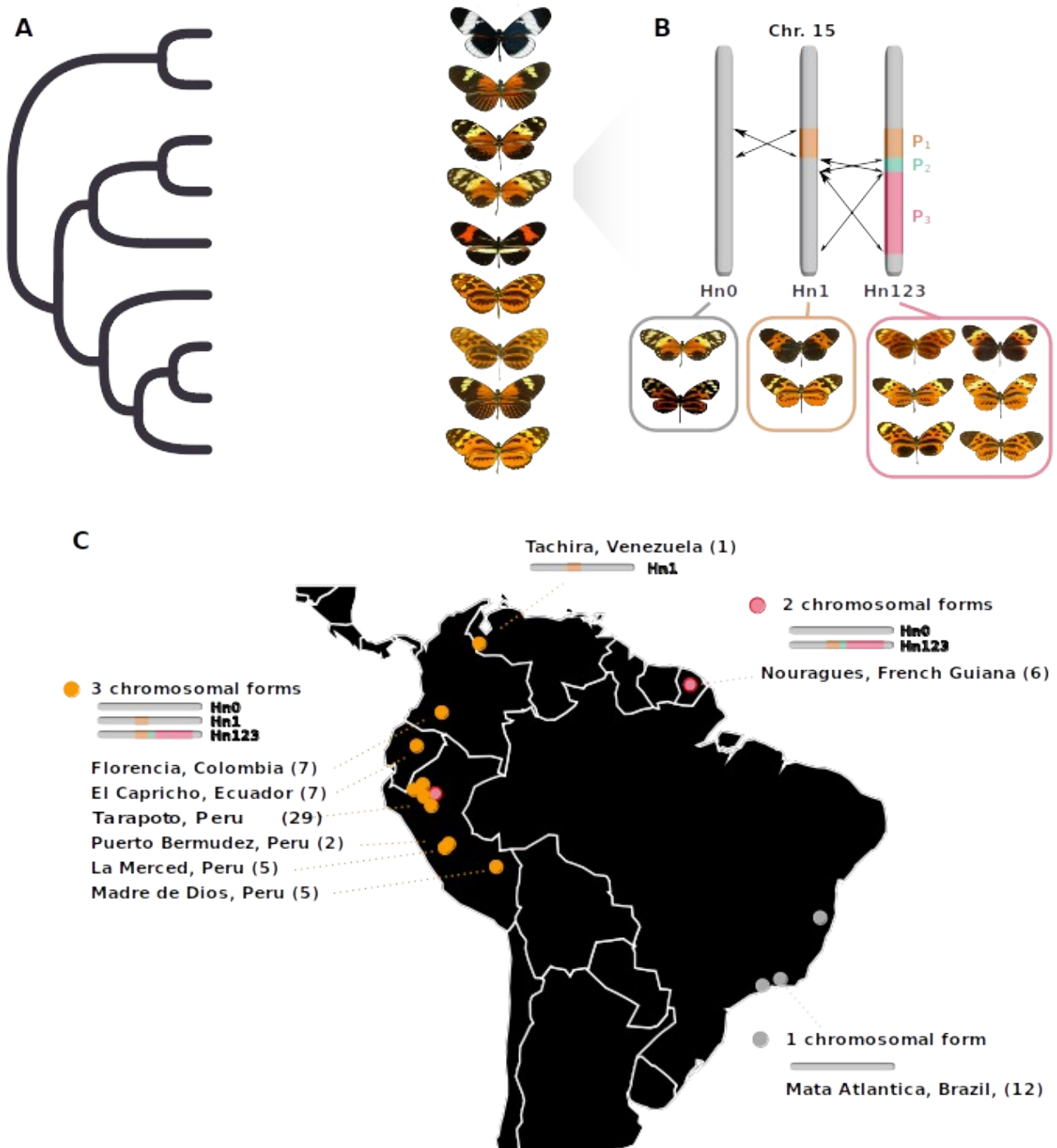
570 **References**

- 571 | 1. Alexander DH, Novembre J, Lange K (2009). Fast model-based estimation of ancestry in
572 | unrelated individuals. *Genome Research* **19**:1655-1664.
- 573 | 2. Alexander, D.H., Lange, K. Enhancements to the ADMIXTURE algorithm for individual ancestry
574 | estimation. BMC Bioinformatics 12, 246 (2011). <https://doi.org/10.1186/1471-2105-12-246>
- 575 | 3. Beichmann AC, Huerta-Sanchez E, Lohmueller KE (2018). Using Genomic Data to Infer
576 | Historic Population Dynamics of Nonmodel Organisms. *Annual Review of Ecology,*
577 | *Evolution, and Systematics* **49**:433–56
- 578 | 4. Benson G (1999) Tandem repeats finder: a program to analyze DNA sequences. *Nucleic*
579 | *Acids Research* **27**:573-580.
- 580 | 5. Brown KS (1979). Ecologia Geográfica e Evolução nas Florestas Neotropicais. – Univ.
581 | Estadual de Campinas, Campinas, Brazil.
- 582 | 6. Brown KS, Benson WW (1974). Adaptive polymorphism associated with multiple müllerian
583 | mimicry in *Heliconius numata* (Lepid.: Nymph.). *Biotropica* **6**:205–228

- 584 7. Brown KS, Mielke OHH. 1972. The Heliconians of Brazil (Lepidoptera: Nymphalidae). Part
585 II. Introduction and general comments, with a supplementary revision of the tribe.
586 *Zoologica, New York*, **57**:1–40.
- 587 8. [Chang CC, Chow CC, Tellier LCAM, Vattikuti S, Purcell SM, Lee JJ \(2015\) Second-](#)
588 [generation PLINK: rising to the challenge of larger and richer datasets. *GigaScience*,](#)
589 [4:s13742–015–0047–8.](#)
- 590 9. Charlesworth B (2009) Fundamental concepts in genetics: effective population size and
591 patterns of molecular evolution and variation. *Nature Reviews Genetics* **10**:195–205.
- 592 10. Chouteau M, Arias M, Joron M (2016). Warning signals are under positive frequency-
593 dependent selection in nature. *Proceedings of the National Academy of Sciences of the USA*
594 **113**:2164–2169.
- 595 11. Chouteau M, Llaurens V, Piron-Prunier F, Joron M. (2017). Polymorphism at a mimicry
596 supergene maintained by opposing frequency-dependent selection pressures. *Proceedings of*
597 *the National Academy of Sciences of the USA* **114**: 8325–8329.
- 598 12. Davey JW, Chouteau M, Barker SL, Maroja L, Baxter SW, Simpson F, et al. (2016). Major
599 Improvements to the *Heliconius melpomene* Genome Assembly Used to Confirm 10
600 Chromosome Fusion Events in 6 Million Years of Butterfly Evolution. *G3* **6**:695–708.
601 doi:10.1534/g3.115.023655
- 602 13. [Danecek P, Adam Auton, Goncalo Abecasis, Cornelis A. Albers, Eric Banks, Mark A.](#)
603 [DePristo, Robert Handsaker, Gerton Lunter, Gabor Marth, Stephen T. Sherry, Gilean](#)
604 [McVean, Richard Durbin and 1000 Genomes Project Analysis Group, The Variant Call](#)
605 [Format and VCFtools, *Bioinformatics*, 2011](#)
- 606 14. DePristo MA, Banks E, Poplin R, Garimella KV, Maguire JR, Hartl C, Philippakis AA, del
607 Angel G, Rivas MA, Hanna M, McKenna A, Fennell TJ, Kernytsky AM, Sivachenko AY,
608 Cibulskis K, Gabriel SB, Altshuler D, Daly MJ (2011). A framework for variation discovery
609 and genotyping using next-generation DNA sequencing data. *Nature Genetics* **43**:491–498.
- 610 15. Eckert CG, Samis KE, Loughheed SC (2008). Genetic variation across species' geographical
611 ranges: the central–marginal hypothesis and beyond. *Molecular Ecology* **17**:1170–1188.
- 612 16. Edelman NB, Frandsen PB, Miyagi M, Clavijo B, Davey J, Dikow RB, García-Accinelli G,
613 Van Belleghem SM, Patterson N, Neafsey DE, Challis R, Kumar S, Moreira GRP, Salazar
614 C, Chouteau M, Counterman BA, Papa R, Blaxter M, Reed RD, Dasmahapatra KK,
615 Kronforst M, Joron M, Jiggins CD, McMillan WO, Di Palma F, Blumberg AJ, Wakeley J,
616 Jaffe D, Mallet J (2019). Genomic architecture and introgression shape a butterfly radiation.
617 *Science* **366**:594–599.
- 618 17. Emsley MG 1965. Speciation in *Heliconius* (Lep., Nymphalidae): morphology and
619 geographic distribution. *Zoologica, New York* **50**:191–254.
- 620 18. Faria R, Johannesson K, Butlin RK, Westram AM (2019). Evolving inversions. *Trends in*
621 *Ecology & Evolution* **34**:239–248.
- 622 19. Freedman AH, Gronau I, Schweizer RM, Ortega-Del Vecchyo D, Han E, et al. (2012)
623 Genome Sequencing Highlights the Dynamic Early History of Dogs. *PLoS Genetics*
624 **10**:e1004016.
- 625 20. Glinka S, Ometto L, Mousset S, Stephan W, De Lorenzo D (2003) Demography and natural
626 selection have shaped genetic variation in *Drosophila melanogaster*: a multi-locus approach.

- 627 *Genetics* **165**:1269-1278.
- 628 21. Gronau I, Hubisz MJ, Gulko B, Danko CG, Siepel A (2011). Bayesian inference of ancient
629 human demography from individual genome sequences. *Nature Genetics* **43**:1031-1034.
- 630 22. Hackenberg M, Previti C, Luque-Escamilla PL, Carpena P, Martínez-Aroza J, Oliver JL.
631 (2006) CpGcluster: a distance-based algorithm for CpG-island detection. *BMC*
632 *Bioinformatics* **7**:446.
- 633 23. Hedrick PW, Tuttle EM, Gonser RA (2018) Negative-Assortative Mating in the White-
634 Throated Sparrow. *Journal of Heredity* **109**:223-231.
- 635 24. *Heliconius* Genome Consortium (2012). Butterfly genome reveals promiscuous exchange of
636 mimicry adaptations among species. *Nature* **487**: 94–8.
- 637 25. Jay P, Whibley A, Frézal L, Rodríguez de Cara MÁ, Nowell RW, Mallet J, Dasmahapatra
638 KK, Joron M. (2018). Supergene evolution triggered by the introgression of a chromosomal
639 inversion. *Current Biology* **28**:1839-1845.
- 640 26. Jay P, Chouteau M, Whibley A, Bastide H, Parrinello H, Llaurens V, Joron M. (2021).
641 Mutation load at a mimicry supergene sheds new light on the evolution of inversion
642 polymorphisms. *Nature Genetics* **53**:288-293.
- 643 27. Jiggins C, Naisbit R, Coe R, Mallet J 2001. Reproductive isolation caused by colour pattern
644 mimicry. *Nature* **411**:302–305.
- 645 28. Joron M, Wynne IR, Lamas G, Mallet J (1999) Variable selection and the coexistence of
646 multiple mimetic forms of the butterfly *Heliconius numata*. *Evol Ecol* **13**: 721–754.
- 647 29. Joron M, Papa R, Beltran M, Chamberlain N, Mavarez J, et al. (2006) A conserved
648 supergene locus controls colour pattern diversity in *Heliconius* butterflies. *PLoS Biology*
649 **4**:e303
- 650 30. Joron M, Frezal L, Jones RT, Chamberlain NL, Lee SF, Haag CR, Whibley A, Becuwe M,
651 Baxter SW, Ferguson L, Wilkinson PA, Salazar C, Davidson C, Clark R, Quail MA,
652 Beasley H, Glithero R, Lloyd C, Sims S, Jones MC, Rogers J, Jiggins CD, ffrench-Constant
653 RH (2011). Chromosomal rearrangements maintain a polymorphic supergene controlling
654 butterfly mimicry. *Nature* **477**:203–206.
- 655 31. Knoppien P (1985) Rare male mating advantage: a review. *Biological Reviews* **60**:81-117.
- 656 32. Lenormand T (2002) Gene flow and the limits to natural selection. *Trends in Ecology and*
657 *Evolution* **17**:183-189.
- 658 33. Lenth RV (2016). Least-Squares Means: The R Package lsmeans. *Journal of Statistical*
659 *Software* **69**:1-33.
- 660 34. Li H, Handsaker B, Wysoker A, Fennell T, Ruan J, Homer N, Marth G, Abecasis G, Durbin
661 R; 1000 Genome Project Data Processing Subgroup (2009). The Sequence Alignment/Map
662 format and SAMtools. *Bioinformatics* **25**:2078-2079.
- 663 35. Lunter G, Goodson M (2011). Stampy: a statistical algorithm for sensitive and fast mapping
664 of Illumina sequence reads. *Genome Research* **21**:936-939.
- 665 36. Maisonneuve L., Chouteau M, Joron M, Llaurens V (2021). Evolution and genetic
666 architecture of disassortative mating at a locus under heterozygote advantage. *Evolution*
667 **75**:149-165.
- 668 37. Mallet J, McMillan W, Jiggins C (1998). Estimating the mating behavior of a pair of
669 hybridizing *Heliconius* species in the wild. *Evolution* **52**:503–510.

- 670 38. Martin SH, Möst M, Palmer WJ, Salazar C, McMillan WO, Jiggins FM, Jiggins CD (2016).
671 Natural Selection and Genetic Diversity in the Butterfly *Heliconius melpomene*. *Genetics*
672 **203**:525-541.
- 673 39. Mitchell-Olds T, Willis JH, Goldstein DB (2007). Which evolutionary processes influence
674 natural genetic variation for phenotypic traits? *Nature Reviews Genetics* **8**:845–856.
- 675 40. Muers, M (2009) Separating demography from selection, *Nature Reviews Genetics* **10**:280–
676 281.
- 677 41. Murray GGR, Soares AER, Novak BJ, Schaefer NK, Cahill JA, Baker AJ, Demboski JR,
678 Doll A, Da Fonseca RR, Fulton TL, Gilbert MTP, Heintzman PD, Letts B, McIntosh G,
679 O'Connell BL, Peck M, Pipes ML, Rice ES, Santos KM, Sohrweide AG, Vohr SH, Corbett-
680 Detig RB, Green RE, Shapiro B (2017). Natural selection shaped the rise and fall of
681 passenger pigeon genomic diversity. *Science* **358**:951-954.
- 682 42. McMillan W, Jiggins C, Mallet J (1997). What initiates speciation in passion-vine
683 butterflies? *Proceedings of the National Academy of Sciences of the USA* **94**:8628–8633.
- 684 43. Nadeau NJ, Pardo-Diaz C, Whibley A, Supple M A, Saenko SV, Wallbank RWR *et al.*
685 (2016). The gene *cortex* controls mimicry and crypsis in butterflies and moths. *Nature*,
686 **534**:106–110.
- 687 44. Nielsen, R., Hubisz, M.J., Hellmann, I., Torgerson, D., Andres, A.M., Albrechtsen, A.,
688 Gutenkunst R, Adams MD, Cargill M, Boyko A, Indap A, Bustamante CD, and Clark AG
689 (2009). Darwinian and demographic forces affecting human protein coding genes. *Genome*
690 *Research* **19**:838–849.
- 691 45. ~~Patterson N, Price AL, Reich D (2006) Population Structure and Eigenanalysis. *PLoS*~~
692 ~~*Genetics* **2**: e190.~~
- 693 46. Rosser N, Phillimore AB, Huertas B, Willmott KR, Mallet J (2012) Testing historical
694 explanations for gradients in species richness in heliconiine butterflies of tropical America.
695 *Biological Journal of the Linnean Society* **105**:479–497.
- 696 47. Schiffels S, Durbin R (2014) Inferring human population size and separation history from
697 multiple genome sequences. *Nature Genetics* **46**:919-925.
- 698 48. Saenko SV, Chouteau M, Piron-Prunier F, Blugeon C, Joron M, Llaurens V (2019)
699 Unravelling the genes forming the wing pattern supergene in the polymorphic butterfly
700 *Heliconius numata*. *EvoDevo* **10**:1-12.
- 701 49. Sheppard PM, Turner JRG, Brown KS, Benson WW, Singer MC (1985) Genetics and the
702 evolution of Muellierian mimicry in *Heliconius* butterflies. *Philosophical Transactions of the*
703 *Royal Society of London, B Biological Sciences* **308**: 433–610
- 704 50. Slatkin M (1987) Gene flow and the geographic structure of natural populations. *Science*
705 **236**:787-792
706



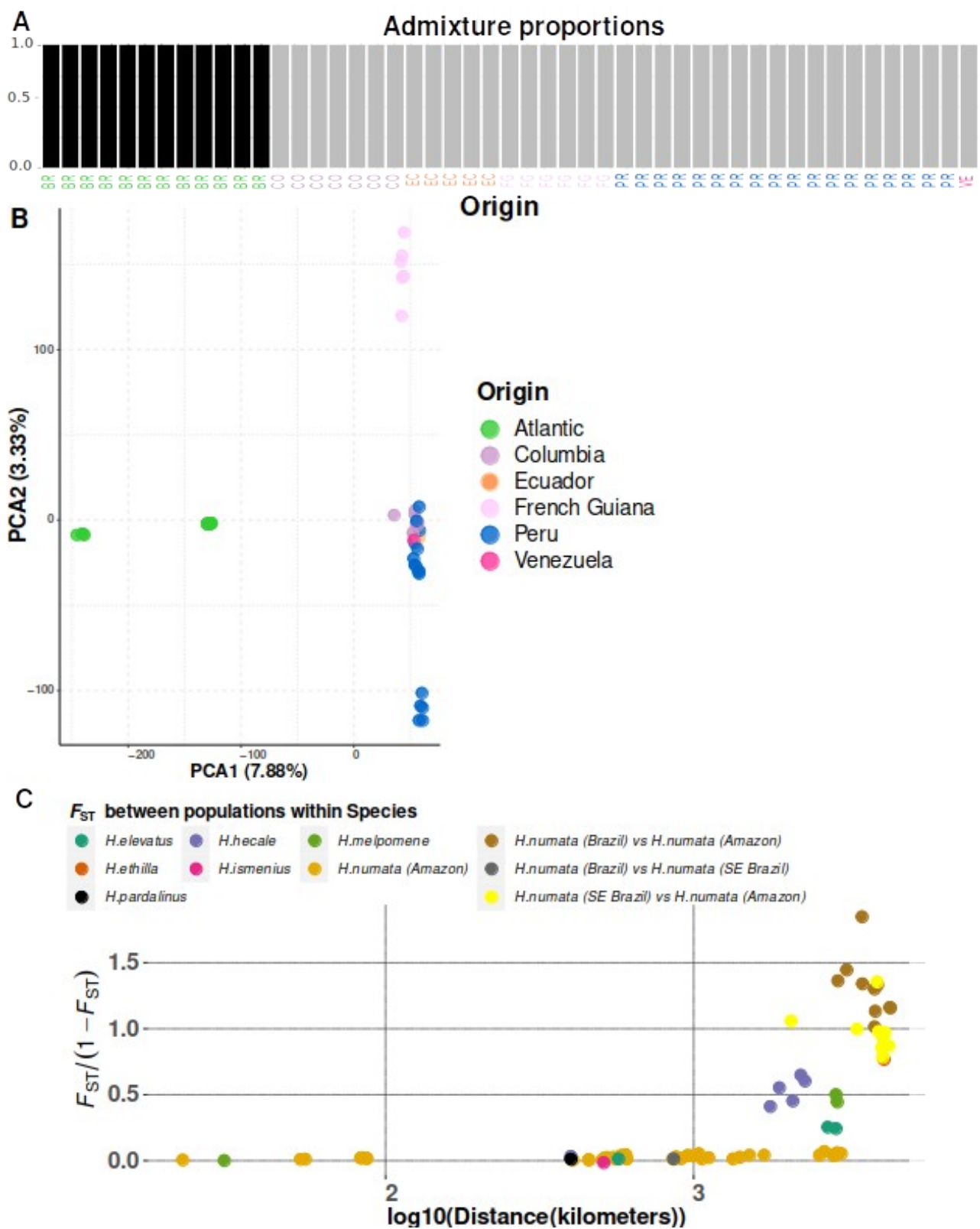
708 **Figure 1 | Genetic and population structure at the P supergene.**

709 **A.** Schematic phylogeny of the sampled species. It includes all members of the silvaniform clade
710 and two outgroups, *H. melpomene* and *H. cydno*.

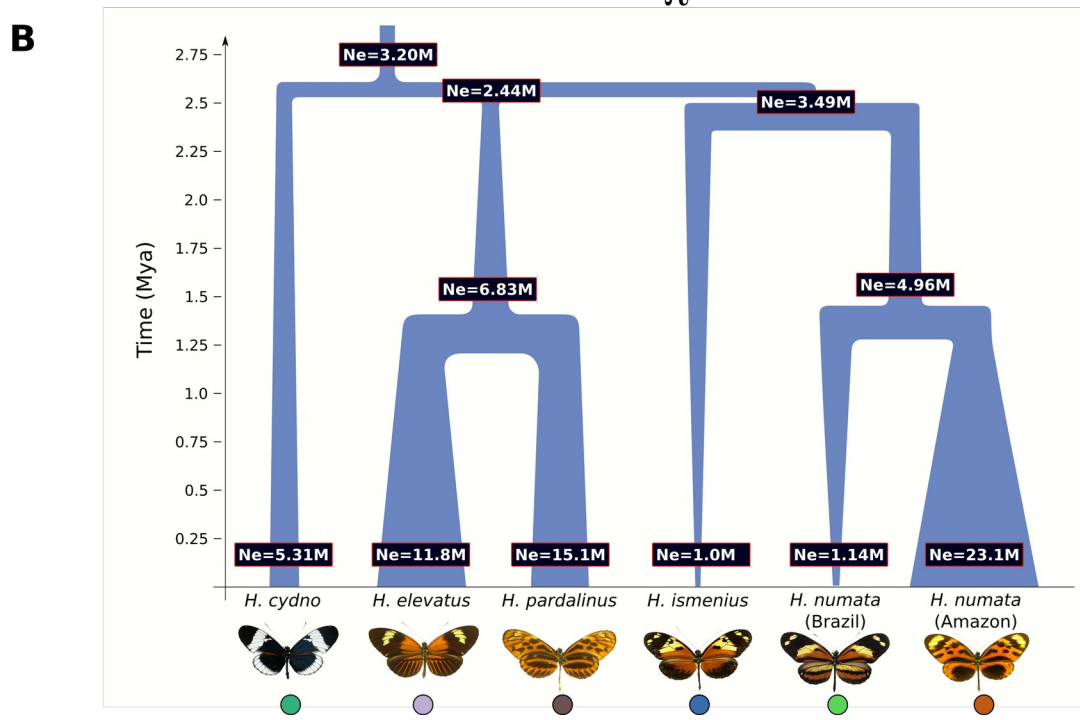
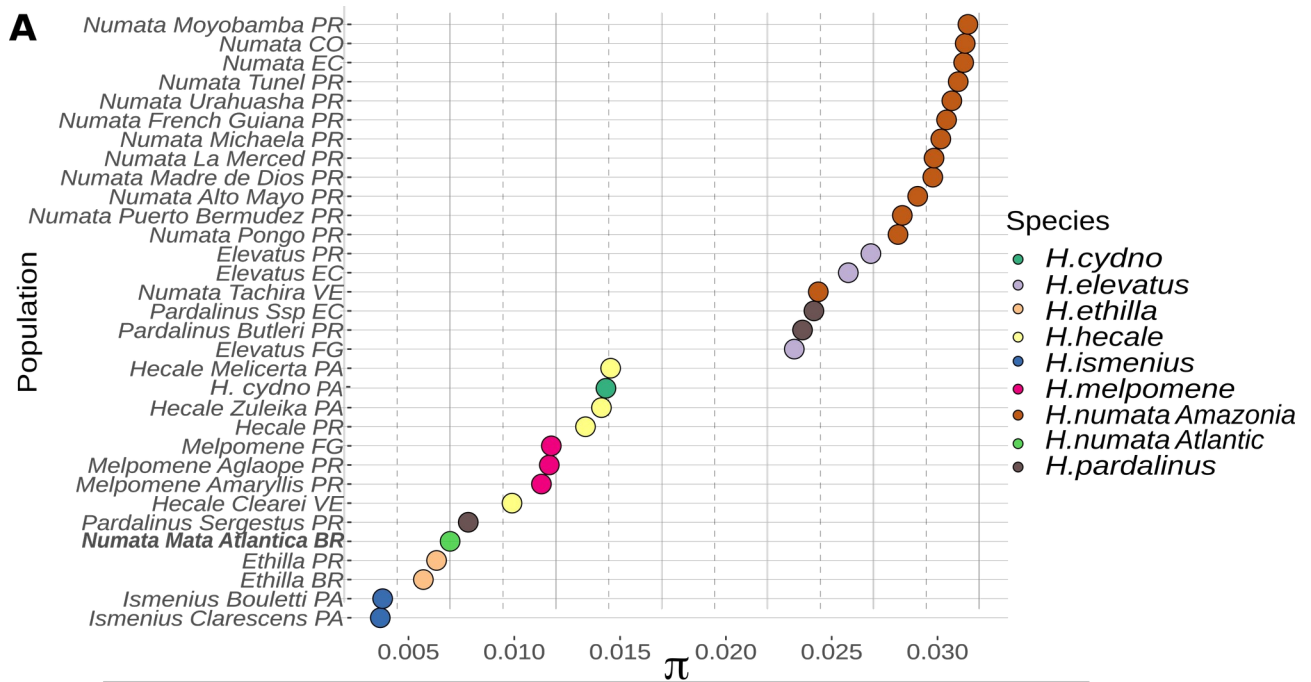
711 **B.** Schematic description of the genetic structure of the P supergene. Three chromosomal
712 arrangements coexist in *H. numata* and are associated with different morphs.

713 **C.** Origin of *H. numata* specimens used for analyses and distribution of chromosome arrangements
714 across the neotropics. Numbers in brackets indicate sampled specimens in each locality (the
715 Tarapoto population lumps several neighbouring subsamples on the map)

716

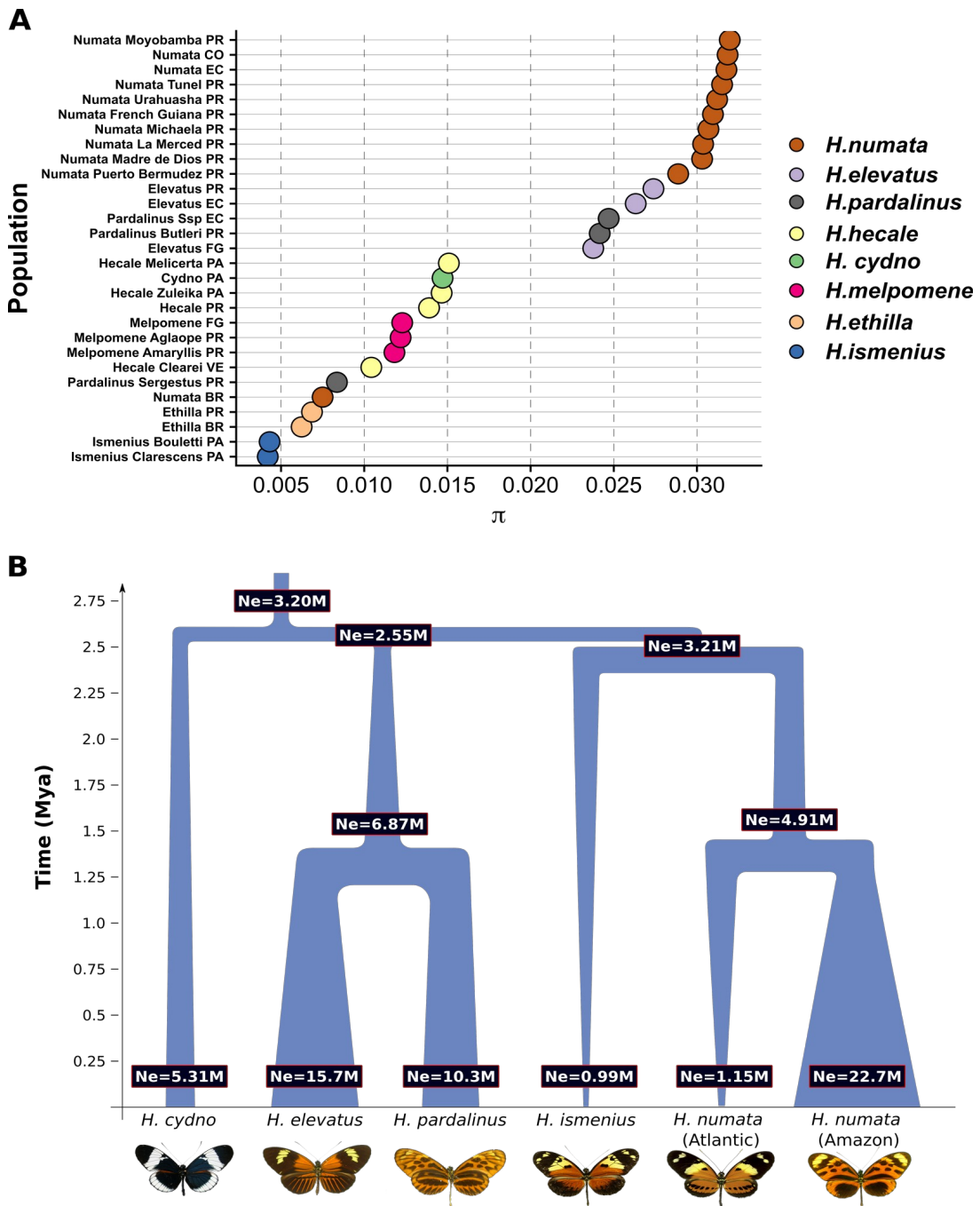


718 **Figure 2 | *H. numata* is characterised by low population structure.**
 719 **A. Admixture plot for *H. numata*. The optimal cluster number for *H. numata* is two, and it splits *H. numata* into**
 720 **two categories, whereas they come from Atlantic forest or the Amazon. BR=Brazil (Atlantic), PR=Peru,**
 721 **VE=Venezuela, CO=Colombia, EC=Ecuador, FG=French Guiana. B. Principal component analysis computed on**
 722 **whole genome SNP. Color code match those given in the admixture label of panel A. C. Relationship between**
 723 **genetic differentiation ($F_{ST}/(1-F_{ST})$) and logarithm of geographical distance. F_{ST} is measured between**
 724 **morphs/populations of the same species. *H. numata* populations from the Amazon show low isolation by distance**
 725 **when compared to related species.:**



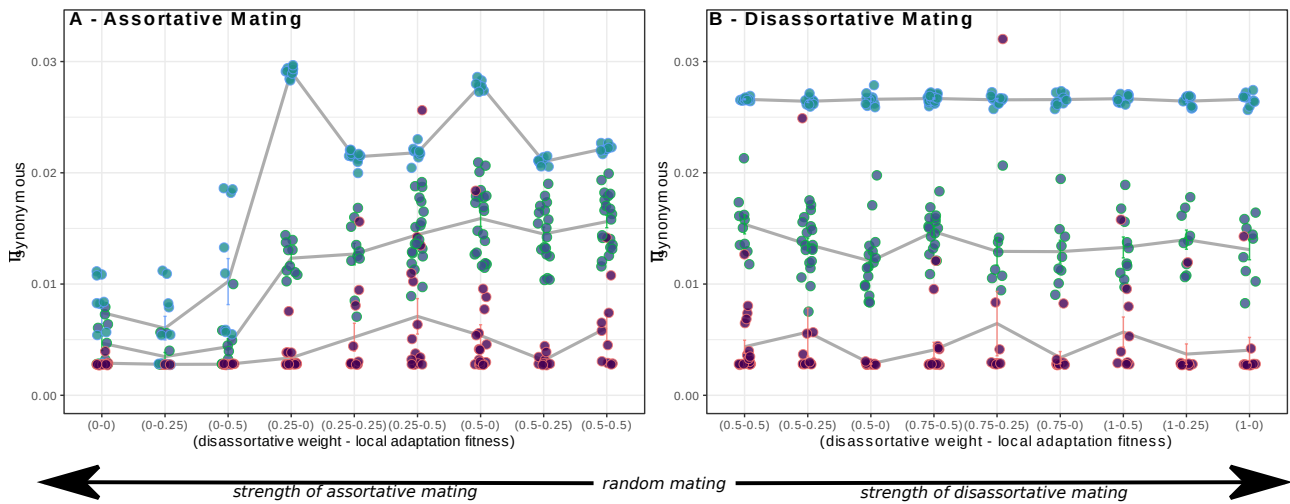
727

728 **Figure 3 | Variation in present and past effective population size in *Heliconius* species**
 729 **A.** Variation in π in several *Heliconius* populations, showing higher genetic diversity in *H.*
 730 *numata* populations from the Amazon than other taxa. Population names indicates their origin as in
 731 Figure 2 (e.g. PR=Peru), with the addition of PA=Panama. The *H. numata* population with a lowest
 732 diversity is the one from the Atlantic forest (Brazil). **B.** Schematic representation of Gphocs results
 733 (presented in table S5-6). Gene flow was modelled but not represented graphically for clarity.
 734 showing that Amazonian populations of *H. numata*, which have the P supergene, show a dramatic
 735 increase in population size posterior to their split with the Atlantic populations of Brazil, which lack
 736 the supergene.



746 **Figure 3 | Variation in present and past effective population size in *Heliconius* species**
 747 **A.** Variation in π in several *Heliconius* populations, showing higher genetic diversity in *H. numata*
 748 populations from the Amazon than other taxa. Population names indicates their origin as in Figure 2
 749 (e.g. PR=Peru), with the addition of PA=Panama. The *H. numata* population with a lowest diversity
 750 is the one from the Atlantic forest (Brazil). **B.** Schematic representation of Gphocs results
 751 (presented in table S5-6). Gene flow was modelled but not represented graphically for clarity.
 752 showing that Amazonian populations of *H. numata*, which have the P-supergene, show a dramatic
 753 increase in population size posterior to their split with the Atlantic populations of Brazil, which lack
 754 the supergene.

755
 756
 757



759 **Figure 4 | Weak but significant differences in synonymous nucleotide diversity (π_s) emerged at**
 760 **a genome-wide scale under divergent selection and mating region.** Results from forward
 761 simulations of 10 populations undergoing local adaptation and different mating strategy are
 762 presented. Shown are levels of synonymous diversity obtained under assortative (A) versus
 763 disassortative mating (B) under different rates of migration and different local adaptation fitness.
 764 Each combination of parameters in brackets display the (dis)-assortative mating weight and the
 765 fitness value for local adaptation respectively. A left value of 0 in the bracket means complete
 766 assortative mating and 0.5 means no assortative mating or disassortative mating. Value of 1 means
 767 complete disassortative mating. A right value of 0 in the bracket mean fitness of 0 for non locally
 768 adapted individuals in a demes, A value of 0.5 means a reduced fitness of 0.5 relative to the
 769 maximum value

770 | **List of Supplementary Materials:**

771 Table S1-6

772 Fig S1-2

773 Text S1

774